

THERMALLY ASSISTED MACHINING PROCESSES

Frank P. Incropera – fpi@nd.edu
College of Engineering
University of Notre Dame
Notre Dame, IN 46556 USA

Abstract. In recent years advanced materials, such as structural ceramics, high-temperature alloys and metal-matrix composites, have increasingly been used to endow products with attributes such as high hardness, large strength-to-weight ratio, and enhanced wear and corrosion resistance. However, stringent dimensional requirements for the finished products commonly preclude reliance on net shape forming processes, and a finishing (machining) operation is needed. When applied to such materials, conventional machining processes suffer from low material removal rates, rapid tool wear and/or severe damage to the workpiece. However, these problems may be mitigated by using a hybrid process termed thermally-assisted machining (TAM), for which an intense heat source is used to thermally condition the workpiece before material is removed by conventional means. In this paper TAM processes are reviewed, with emphasis placed on the development of process models and significant trends revealed by predictions for representative operating conditions.

Keywords: Thermally assisted machining, Lasers, Ceramics.

1. INTRODUCTION

Although forming processes can produce different shapes at high production rates, the attendant dimensional accuracy and surface finish are often unacceptable and a finishing (machining) operation is required. However, although traditional machining processes, which involve use of a cutting tool to induce mechanical stresses in excess of the yield strength, are well suited for ductile materials, many modern materials are difficult to machine and in some cases unmachinable by conventional methods.

1.1 Difficult-to-machine materials and machining methods

Difficult-to-machine materials include most ceramics and selected alloys and composites. The poor machinability of Ti, Ni and Co-based alloys is due to their propensity to strain-harden during the severe plastic deformation induced by single-point cutting tools. Hence, conventional machining techniques suffer from rapid tool wear and low machining speeds.

Common structural ceramics that are difficult to machine by conventional methods include silicon nitride (Si_3N_4), silicon carbide (SiC), zirconia (ZrO_2), alumina (Al_2O_3), mullite ($3\text{Al}_2\text{O}_3 \cdot 2\text{SiO}_2$) and cermets such as tungsten and carbide (WC). Application of conventional single point machining methods to such materials is limited by their inherent brittleness, which requires material removal by fracture rather than plastic deformation. Accordingly, there is severe damage to the surface of the workpiece, as well as rapid tool failure.

In lieu of using single-point cutting, difficult-to-machine materials may be shaped by abrasive, non-contact or hybrid machining methods. Grinding is the most commonly used abrasive method and is capable of achieving excellent dimensional accuracy and surface finish. However, it is limited to low material removal rates and can create residual stresses and subsurface cracks that are not removable in a finishing operation. Non-contact machining involves exposure of the workpiece to an intense energy source, such as a laser, electron or ion beam, and material removal by melting and vaporization. However, material removal rates are low, and thermal stresses and cracks induced by intense heating reduce part strength.

In a hybrid process, such as thermally assisted machining (TAM), an intense heat source is used to thermally condition a workpiece before material is removed by a cutting tool. The objective is to reduce the yield strength of the material by intense local heating before it is removed by a cutting tool. For example, the yield stress and strain hardening of a Ni-based alloy could be reduced by intense local heating, thereby increasing the material removal rate and reducing tool wear. Similarly, by heating a structural ceramic, it may become ductile and material removal may be effected by plastic deformation, rather than brittle fracture.

1.2 Feasibility of TAM

The first studies of TAM were performed approximately 50 years ago and involved the use of an oxyacetylene torch or an induction coil to preheat hard metals prior to machining (Schmidt, 1949; Krabachar and Merchant, 1951). Although reductions in tool loads with increasing workpiece temperature were reported, the intensity and region of heating were not easily controlled.

A variant of TAM that permits greater control over the heating location and intensity involves using a plasma torch as the heat source. The method was proposed by Moore (1977) and has been applied to ceramics (Kitagawa and Mackawa, 1990), as well as to Inconel 718 (Novak et al., 1997). Reduced cutting forces and tool wear, as well as improved surface finish, were reported, although workpiece fracture due to thermal stresses was observed for zirconia and alumina.

In recent years TAM activities have focused on using lasers to enable application of conventional machining operations (turning and milling) to ceramics. König and Wagemann (1991) and König and Zaboklicki (1993) found that quasi-plastic deformation could be achieved in Si_3N_4 by preheating the workpiece to approximately 1100°C, with significant reductions in cutting forces and tool wear. They also concluded that material removal is effected by the softening of amorphous phases at Si_3N_4 grain boundaries. The conclusion was also reached by Rozzi et al. (1998a), whose experiments involved Si_3N_4 sintered with YSiAlON. The sintering agent has a glass transition temperature of approximately 950°C, which corresponded to the lower bound for effective material removal in their experiments.

Lei et al. (1999) also performed experiments for laser-assisted machining of Si_3N_4 and found that the tool wear rate decreased significantly with increasing material removal temperature from

1260°C to 1410°C, but that, above a threshold temperature, increased tool wear, if not tool fracture, would occur. The surface roughness of the machined workpiece was approximately 0.5 μ m, and no sub-surface cracks were observed.

1.3 Thermal Conditions

To develop a complete understanding of conditions associated with TAM and to facilitate determination of optimal operating conditions, a thermal model of the process is needed. The first steps in developing such a model were taken by Rozzi et al. (1998b, c), who considered the thermal response of a rotating cylindrical workpiece (Si_3N_4) heated by a CO_2 laser beam. Good agreement was obtained between predictions and measurements of the surface temperature, and parametric variations of laser operating conditions were considered. Numerical predictions of the transient, three-dimensional model were also used to assess the accuracy and limitations of a simplified two-dimensional model.

The foregoing model was extended by Rozzi et al. (2000a, b) to include the effects of material removal due to machining, and once again measured surface temperatures were in good agreement with the predictions. The temperature field in the workpiece was most strongly influenced by the laser power and axial, laser-tool lead distance, as well as by the laser/tool translational velocity. Thermal energy generation in the primary shear zone associated with material removal had a significant influence on material removal temperatures, while the effects of friction at the tool-flank interface were negligible.

Silicon nitride is an opaque ceramic for which radiative transfer is exclusively a surface phenomenon. However, ceramics such as alumina, zirconia and mullite are semi-transparent, and at the elevated temperatures associated with TAM, volumetric radiation emission, absorption and scattering within the workpiece can have a significant influence on thermal conditions. Although Pfefferkorn et al. (1999) used the diffusion approximation to account for internal radiative transfer in modeling laser-assisted machining for partially stabilized zirconia, the assumption was found to be inadequate for certain regions of the spectrum.

2. MATHEMATICAL MODEL: LASER-ASSISTED TURNING

A laser-assisted turning operation involves laser irradiation of a cylindrical workpiece near the material removal location, and conditions associated with an intermediate stage of machining are shown in Fig. 1. Relative to the incident laser radiation and the cutting tool, motion of the workpiece is characterized by rotation and translation in the circumferential and axial directions, respectively. The boundary between machined and unmachined portions of the workpiece is represented by a helical chamfer, on which the small $r - z$ plane at $f = 0$ corresponds to the location of material removal. The location of the cutting tool relative to the center of the laser spot is designated by the parameters f_t and L_f , where L_f extends to the outermost edge of the material removal plane. To facilitate a numerical solution of the temperature field, the material removal plane is approximated as a rectangle of depth d and width L_f , which corresponds to a hypothetical cutting tool of zero lead angle ($\Omega_t = 0$) and radius ($r_t = 0$), with the chamfer located at the average distance between the edge of the material removal plane and the center of the laser spot.

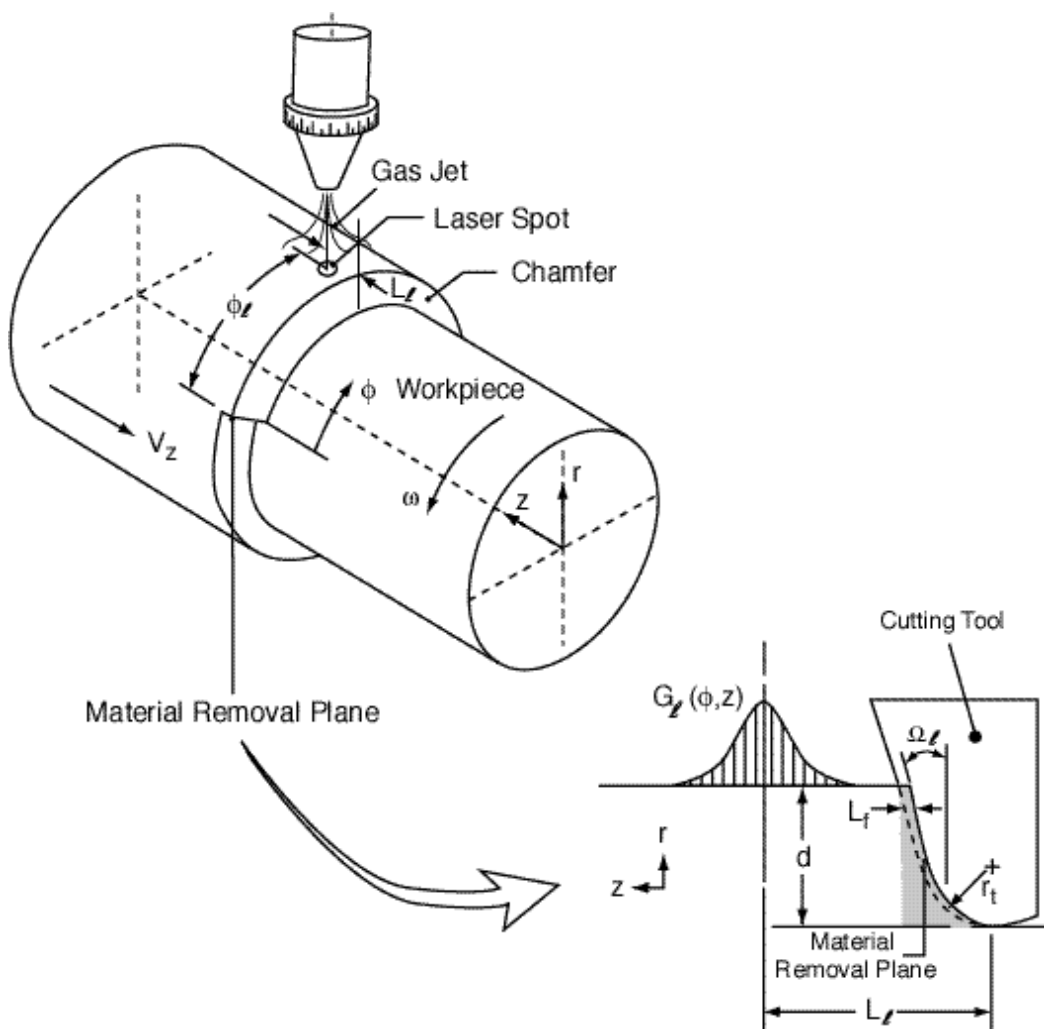


Figure 1 – Schematic of laser-assisted turning.

A comprehensive model for predicting the transient, three-dimensional temperature field associated with laser-assisted turning should include: (i) localized heating due to laser irradiation; (ii) radiation emission from the surface of the workpiece and, for semi-transparent ceramics, volumetric emission, absorption and scattering of radiation within the workpiece; (iii) heat transfer by forced convection from the irradiated portion of the surface to a gas jet which is coaxial with the laser beam (Fig. 1); (iv) heat transfer to quiescent ambient air by mixed convection from a rotating surface; (v) thermal energy generation due to plastic deformation within the zone associated with material removal; (vi) surface heating due to friction at the interface between the tool flank and the workpiece; (vii) three-dimensional conduction within the workpiece; and (viii) advection associated with workpiece rotation and linear movement of the workpiece relative to the laser and cutting tool.

A requisite and complicating feature of such a model relates to geometrical characterization of the chamfered and material removal surfaces which separate machined and unmachined portions of the workpiece. In a turning operation, the tool has a single cutting edge and material removal is continuous. A related complexity concerns geometrical characterization of the

primary shear zone, within which strain rates and plastic deformation are extremely large. The volumetric rate at which work is done in this zone provides the mechanical equivalent of heat generation.

The energy equation which characterizes thermal conditions within the workpiece may be expressed as

$$\mathbf{r}c_p \left(\frac{\partial T}{\partial t} + \mathbf{w} \frac{\partial T}{\partial \mathbf{f}} + V_z \frac{\partial T}{\partial z} \right) = \frac{1}{r} \frac{\partial}{\partial r} \left(kr \frac{\partial T}{\partial r} \right) + \frac{1}{r^2} \frac{\partial}{\partial \mathbf{f}} \left(k \frac{\partial T}{\partial \mathbf{f}} \right) + \frac{\partial}{\partial z} \left(k \frac{\partial T}{\partial z} \right) + \dot{q}_{pd} + \dot{q}_r \quad (1)$$

The terms on the left-hand side of the equation represent the inherently transient nature of TAM and advection due to relative motion between the workpiece and the laser/tool in the circumferential and axial directions. The first three terms on the right-hand side of the equation account for conduction in the workpiece, while the fourth term is a volumetric source of thermal energy due to plastic deformation in the primary shear zone. The fifth term, which represents the net rate at which thermal energy is generated due to radiation absorption and emission, must be included if the workpiece is semi-transparent.

With requisite temperatures for plastic deformation exceeding 1000 C, internal radiation emission, absorption and scattering will occur in ceramics such as alumina and zirconia (Makino et al., 1984). The net rate at which radiation is absorbed per unit volume and time over wavelengths for which the material is semi-transparent may be expressed as (Özisik, 1973)

$$\dot{q}_r = \int_{\Delta I} \left[\mathbf{k}_I \int_{4p} I_I(s, \hat{\Omega}') d\Omega' - 4p \mathbf{k}_I I_{I,b}(T) \right] dI \quad (2)$$

where ΔI designates that portion of the spectrum over which the workpiece is semi-transparent. The spectral intensity, $I_I(s, \hat{\Omega})$, of the radiation field within the workpiece is obtained by solving the radiative transfer equation

$$\frac{dI_I(s, \hat{\Omega})}{ds} = -\mathbf{b}_I I_I(s, \hat{\Omega}) + \mathbf{k}_I I_{I,b}(T) + \frac{\mathbf{s}_I}{4p} \int_{4p} p_I(\hat{\Omega}' \cdot \Omega) I_I(s, \hat{\Omega}') d\Omega' \quad (3)$$

In principle, the volumetric rate of thermal energy generation due to plastic deformation in the material removal region, \dot{q}_{pd} , may be determined from knowledge of the local strain rate $\dot{\epsilon}$ and flow stress \mathbf{s} . In practice, however, conditions in this region are extremely complex, with strain rates as large as $10^4 s^{-1}$.

Numerous models have been developed to simulate thermo-mechanical conditions associated with material removal. With few exceptions, the models are two-dimensional. One approach involves the use of simplified *shear plane* or *shear zone* models, which restrict plastic deformation to a single plane or a thin zone, respectively. A second, more contemporary approach involves use of finite-element methods and treatment of the workpiece as a viscoplastic material for which the local flow stress is a function of the local strain, strainrate and temperature. Implementation of the method requires a constitutive relation linking \mathbf{s} to \mathbf{e} , $\dot{\epsilon}$

and T . With such a relation, the average value of volumetric heat generation in a material removal zone of volume ∇ may be expressed as

$$\dot{q}_{pd} = \frac{\mathbf{f}\dot{E}_s}{\nabla} = \frac{\mathbf{f}}{\nabla} \int_{\nabla} \dot{\mathbf{e}}\mathbf{s} d\nabla \quad (4)$$

where \mathbf{f} represents the fraction of the power requirement \dot{E}_s which is converted to thermal energy, with the remainder stored as latent (strain) energy in the deformed chip. However, although constitutive relations have been obtained for ductile materials at low temperatures, they do not exist for ceramics at the elevated temperatures of TAM. Nevertheless, assuming the total cutting power ($F_c \bar{V}_w$), to be dissipated in material deformation (\dot{E}_s) and friction along the tool rake face ($F_{ct} V_{ch}$), the following expression may be used to estimate volumetric heating in a plastic deformation region of volume ∇ (Rozzi, 2000a).

$$\dot{q}_{pd} = \frac{\mathbf{f}(F_c \bar{V}_w - F_{ct} V_{ch})}{\nabla} \quad (5)$$

where $\mathbf{f} \approx 0.85$, $\nabla \approx dL_f^2 / 10$ and the quantities F_c , F_{ct} and V_{ch} may be determined directly or inferred from measurement of the cutting, feed and thrust force components associated with machining.

The boundary condition at the *unmachined* portion of the cylindrical surface may be expressed as

$$k \frac{\partial T}{\partial r} \Big|_{r=r_w} = \mathbf{a}_\ell G_\ell(\mathbf{f}, z) - q_{cnv} - E(T) \quad (6)$$

where the spatial distribution of the laser irradiation over the workpiece surface, $G_\ell(\mathbf{f}, z)$, is determined by the beam profile. For the majority of the workpiece surface which is not irradiated, this term is absent. The heat flux q_{cnv} is associated with forced convection to a gas jet which impinges on the workpiece in proximity to the laser spot and protects the focusing optic from machining debris or with mixed convection from portions of the surface which are not exposed to the jet.

Formulation of the radiation term $E(T)$ depends on whether the workpiece is opaque or semi-transparent. The boundary condition also applies at the machined portion of the workpiece, which may also be irradiated if the laser spot overlaps the chamfer. However, differences in the unmachined and machined surface conditions may yield different values of the radiative properties. Additional boundary conditions relate to symmetry at the centerline, balances between axial conduction and convection/radiation at the end and chamfered surfaces of the workpiece, symmetry constraints or a balance between advection and conduction for the circumferential direction, and reflection of internal radiation at the surface of the workpiece (for a semi-transparent medium).

3. THEORETICAL RESULTS

Representative results are presented for an opaque silicon nitride workpiece of 8.46 mm diameter and irradiation from a CO₂ laser. The process occurs in two stages, the first of which corresponds to a preheat time t_p for which there is no machining. When temperatures are sufficiently large to prevent tool or workpiece fracture, translational motion of the laser/tool initiates the second stage for $t > t_p$.

Representative comparisons between predictions and measurements are shown in Fig. 2, which provides a comparison of measured and predicted surface temperature histories.

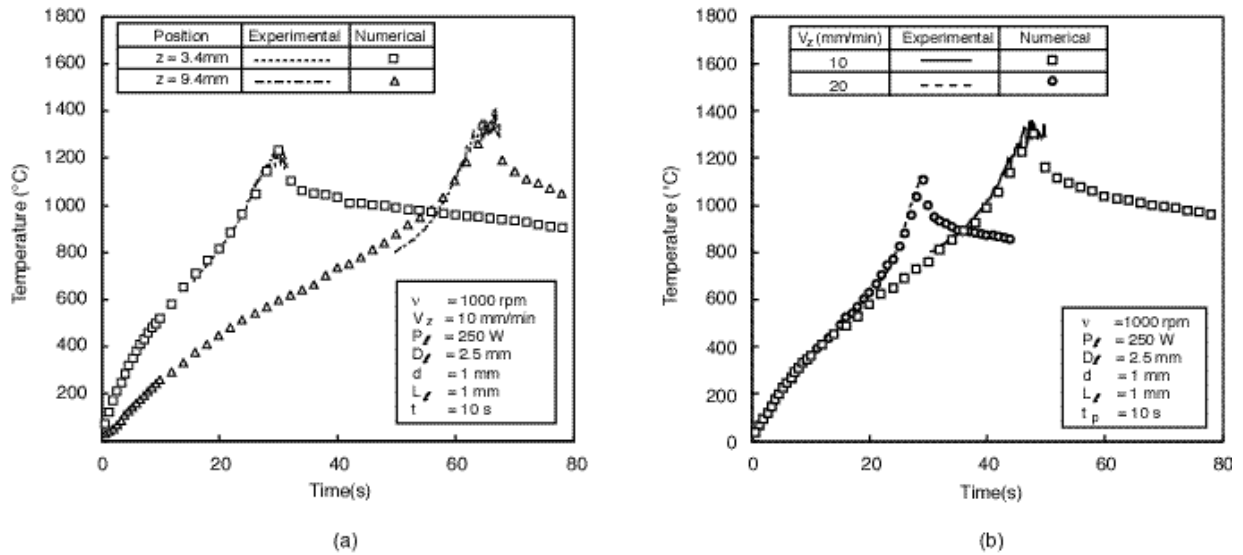


Figure 2 – Surface temperature histories for laser-assisted machining of silicon nitride: (a) effect of axial location, (b) effect of laser/tool translational velocity.

Referring to Fig. 2a, the increase in temperature preceding movement of the laser past the measurement location is due to axial conduction in the workpiece, and the maximum is due to movement of the laser across the $r-f$ plane of the measurement location. The subsequent decay is due to convection and radiation from the surface, as well as conduction in the workpiece. The increase in the maximum with increasing z is due to the increased duration of heating prior to movement of the laser across the measurement location, although quasi-steady conditions are approached for which there would be no further variation in the maximum. As shown in Fig. 2b, the maximum temperature decreases with increasing laser/tool velocity, and there is an upper limit to V_z , beyond which temperatures are less than the minimum value required for successful machining.

For the operating conditions identified in Fig. 2a, the surface temperature distribution is shown in Fig. 3 at $t=40$ s into the machining process. The primary maximum corresponds to the center of the laser spot on the unmachined workpiece surface, and the secondary maxima are associated with energy generation in the primary shear zone and irradiation of the machined portion of the workpiece, which has a lower absorptivity than the unmachined surface. The sharp peak associated with plastic deformation is due to the small volume of the primary shear zone. However, despite the pronounced maxima associated with laser heating and material removal, conduction provides a nearly uniform circumferential temperature distribution at axial

locations which are approximately 2mm beyond the locations of the laser spot and material removal.

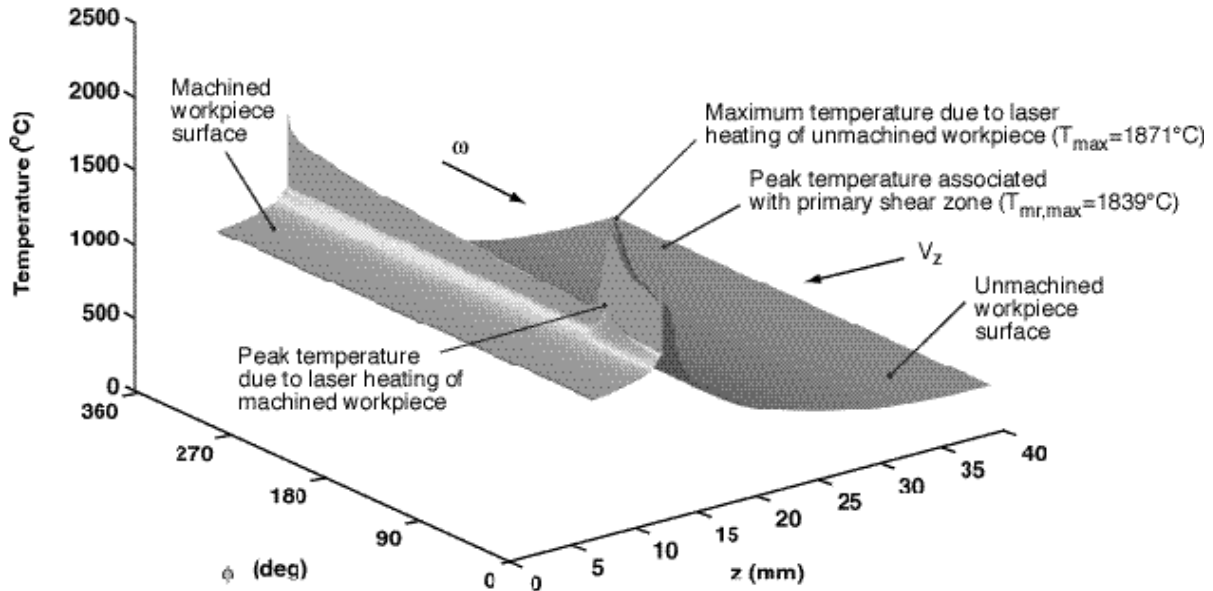


Figure 3 – Surface temperature distribution for laser-assisted machining of silicon nitride ($t=40s$).

The temperature distribution in a longitudinal section that passes through the material removal zone is shown in Fig. 4. Large radial temperature gradients exist within the material removal zone. It is essential that temperatures throughout this zone exceed the minimum allowable temperature for machining of the ceramic.

4. SUMMARY

As efforts to commercialize TAM processes evolve, there will be a growing need for reliable process models, which may be used to determine optimal operating conditions and to establish guidelines for on-line process control. However, uncertainties in requisite material properties limit the extent to which the models may be used for accurate predictions of workpiece thermal behavior. Although there is an extensive data base for the temperature-dependent thermophysical and radiative properties associated with materials of interest, the effects of changing physical and/or chemical states due to the large temperature excursions associated with TAM are largely unknown. Another deficiency in the knowledge base relates to the constitutive stress-strain-strain rate-temperature relations needed to compute heat generation in the material removal zone. Progress must be made in removing these limitations if accurate prediction tools are to be developed for all materials and operating conditions of interest.

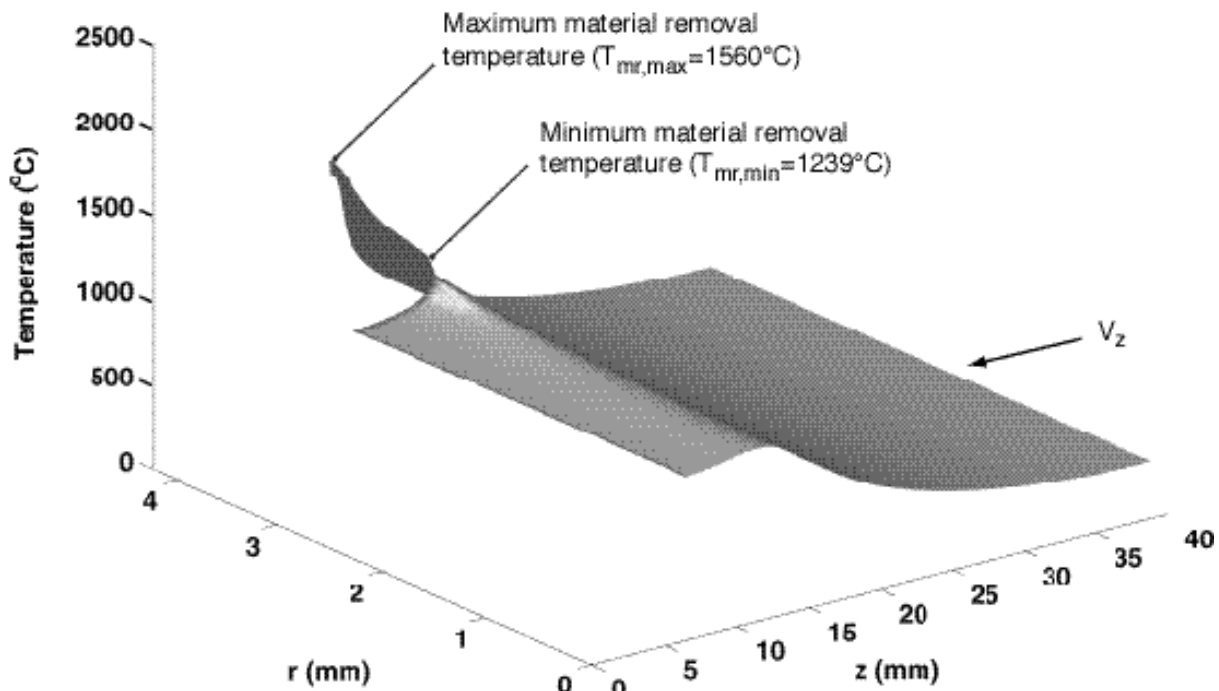


Figure 4 – Temperature distribution in a longitudinal plane passing through the material removal zone ($t = 40s$).

Acknowledgements

Support of this work by the U.S. National Science Foundation under Grant CTS-9802047 is gratefully acknowledged, as are the contributions of Drs. Yung Shin, Jay Rozzi and Shuting Lei and Messrs. Frank Pfefferkorn and Patrick Rebro.

REFERENCES

- Kitagawa, T. & Maekawa, K., 1990, Plasma hot machining for new engineering materials, Wear, vol. 139, pp. 251-267.
- König, W. & Wagemann, J., 1991, Fine machining of advanced ceramics, Proc. 7th Int. Mtng. on Modern Ceramics Technologies, Montecatini, Italy, vol. D, pp. 2769-2783.
- König, W. & Zaboklicki, A.K., 1993, Machining of ceramics components: Process technological potentials, Proc. Int. Conf. on Machining of Advanced Materials, Gaithersburg, MD, NIST Special Publication 847, pp. 3-16.
- Krabacher, E.J. & Merchant, M.E., 1951, Basic factors in hot machining of metals, ASME Transactions, vol. 73, pp. 761-776.

Lei, S., Shin, Y.C. and Incropera, F.P., 1999, Experimental investigation of thermo-mechanical characteristics in laser-assisted machining of silicon nitride ceramics, Proc. ASME IMECE, MED-vol. 10, pp. 761-788.

Makino, T., Kunitomo, T., Sakai, I. and Kinoshita, H., 1984, Thermal radiation properties of ceramic materials, Heat Transfer-Japanese Research, vol. 13, pp. 33-50.

Novak, J.W., Shin, Y.C. and Incropera, F.P., 1997, Assessment of plasma enhanced machining for improved machinability of Inconel 718, ASME Journal of Manufacturing Science and Engineering, vol. 119, pp. 125-129.

Özisik, M.N., 1973, Radiative transfer and interaction with conduction and convection, Wiley, New York.

Pfefferkorn, F.E., Incropera, F.P. and Shin, Y.C., 1999, Transient, three-dimensional heat transfer model for partially stabilized zirconia undergoing laser-assisted machining, Proc. ASME IMECE, HTD vol. 364-3, pp. 197-209.

Rozzi, J.C., Pfefferkorn, F.E., Incropera, F.P. and Shin, Y.C., 1998a, Experimental evaluation of the laser-assisted machining of silicon nitride ceramics, Proc. ASME IMECE, vol. MED-8, pp. 229-239.

Rozzi, J.C., Pfefferkorn, F.E., Incropera, F.P. and Shin, Y.C., 1998b, Transient thermal response of a rotating cylindrical silicon nitride workpiece subjected to a translating laser heat source: I - Comparison of surface temperature measurements with theoretical results, ASME J. Heat Transfer, vol. 120, pp. 899-906.

Rozzi, J.C., Incropera, F.P. and Shin, Y.C., 1998c, Transient thermal response of a rotating cylindrical silicon nitride workpiece subjected to a translating CO₂ laser heat source: II - parametric effects and assessment of a simplified model, ASME J. Heat Transfer, vol. 120, pp. 907-915.

Rozzi, J.C., Pfefferkorn, F.E., Incropera, F.P. and Shin, Y.C., 2000, Transient, three-dimensional heat transfer model for laser assisted machining of silicon nitride: I. Comparison of predictions with measured surface temperature histories, Int. J. Heat Mass Transfer, vol. 43, pp. 1409-1424.

Rozzi, J.C., Incropera, F.P. and Shin, Y.C., 2000, Transient, three-dimensional heat transfer model for the laser assisted machining of silicon nitride: II. Assessment of parametric effects, Int. J. Heat Mass Transfer, vol. 43, pp. 1425-1437.

Schmidt, A.O., 1949, Hot milling-Milling high strength alloys at elevated temperatures, Iron Age, April 28, pp. 66-70.